Efficient Impulsive Noise Suppression based on Statistical Confidence Limits

José Camacho, Samuel Morillas and Pedro Latorre

Instituto de Automática e Informática Industrial, Universidad Politécnica de Valencia, Camino de Vera s/n, C.P. 46022, Valencia, Spain E-mail: jcamacho@isa.upv.es

Abstract. Probably, the most well-known vector filter is the vector median filter (VMF) which is based on the theory of robust statistics and performs good noise suppression in color images. However, the VMF is designed to perform a fixed amount of smoothing. This may lead to too much unnecessary substitutions in the input image and, as a result, blurring and loss of image details. In order to avoid this drawback when dealing with impulsive noise, the switching schemes aim at selecting a set of pixels of the input image to be filtered leaving the rest of the pixels unchanged. In this paper, two switching filters which base the selection of the noisy pixels to be filtered on statistical tests are proposed. The proposed filters present good noise suppression while preserving fine image details appropriately. Comparisons to classical and recently introduced impulsive noise multichannel filters are provided. Moreover, the noisy pixel selection techniques are computationally simple, and the filters significantly reduce the computational complexity of the VMF. © 2006 Society for Imaging Science and Technology.

[DOI: 10.2352/J.ImagingSci.Technol.(2006)50:5(427)]

INTRODUCTION

A well-known nonlinear vector filtering method is based on the ordering of vectors in a predefined sliding window.¹ The most commonly used and more adequate¹ ordering principle between vectors is the reduced ordering principle, which takes advantage of the theory of robust statistics.^{2,3} When the vectors are ranked using the reduced ordering principle by means of a suitable *distance or similarity measure*, the lowest ranked vectors are those which are close to all the other vectors in the window according to the distance or similarity measure used. On the other hand, atypical vectors, susceptible to be considered as noisy or outliers, occupy the highest ranks. The output of these filters is defined as the lowest ranked vector as follows.¹

Let **F** represent a multichannel image and let W be a window of finite size N. The image vectors in the sliding window W are denoted as \mathbf{F}_j , $j=1,\ldots,N$. Let ρ denote an appropriate *distance measure* such that the *distance* between two vectors \mathbf{F}_k , \mathbf{F}_j is denoted as $\rho(\mathbf{F}_k,\mathbf{F}_j)$. For each vector in the filtering window, a global or accumulated distance to all the other vectors in the window has to be calculated. The scalar quantity $R_k = \sum_{j=1,j\neq k}^N \rho\left(\mathbf{F}_k,\mathbf{F}_j\right)$, is the accumulated distance associated to the vector \mathbf{F}_k . The ordering of the R_k 's: $R_{(1)} \leq R_{(2)} \leq \cdots \leq R_{(N)}$, implies the same ordering of the vec-

tors \mathbf{F}_{k} 's: $\mathbf{F}_{(1)} \leq \mathbf{F}_{(2)} \leq \cdots \leq \mathbf{F}_{(N)}$. Given this order, the output of the filter is $\mathbf{F}_{(0)}$.

The above concept is employed by the vector median filter (VMF), ⁴ the basic vector directional filter, ⁵ and the distance directional filter ⁶ which use the aggregated Euclidean distance, the aggregated angular distance, and the aggregated hybrid measure as the ordering criterion, respectively. The interested reader can find extensive information in Ref. 7 which is the most recent overview in the area of color image filtering.

Since these filters produce a fixed amount of smoothing, they usually remove fine details and blur structural information in the image. Therefore, a number of detail-preserving color image filters, such as those based on weighted filtering, ^{8–11} fuzzy logic, ^{1,12–16} and switching filtering concepts ^{17–21,24,25} have been proposed recently.

It must be stressed that some weighted filters and fuzzy logic strategies can be adapted for the suppression of noise with different distributions whereas switching filters are mainly aimed at filtering in an environment corrupted by impulsive noise. In such cases, switching filters are widely used due to their sufficient performance and proven computational simplicity.

Within all this context, several switching mechanisms have been proposed. In Ref. 22, an approximation of the variance based on the minimum aggregated Euclidean distance or on the aggregated Euclidean distance to the multichannel sample mean is used to obtain a threshold to detect noisy pixels. Privileging each pixel to substitute it only when it is considered as a noisy pixel is proposed in Refs. 13, 17, 18, and 21. The use of cluster analysis to select the noisy pixels is proposed in Ref. 19. A fuzzy noise detection technique is introduced in Ref. 16. In Ref. 14, a genetic algorithm is used to decide the switching operation. The filters in Refs. 20 and 23 use the standard deviation, the sample mean and various distance measures to form the adaptive switching rule. In the approaches introduced in Refs. 24 and 25, a neighborhood test is used to decide the switching operation.

In this paper, two fast methods based on statistical confidence limits to detect the pixels in the image which are likely to be noisy are introduced as the switching mechanisms between the identity operation and the VMF operation. The VMF operation will be applied only for those

pixels selected by the test. Thus, the uncorrupted image structures will be better preserved and the filtering process will be more computationally efficient than the classical VMF.

NOISY PIXELS SELECTION AND FILTERING

In a multichannel image, each pixel is represented as a vector $\mathbf{x} \in X^d$, with d the number of channels of the image (for RGB color images, d=3 and $X=\{0,1,\ldots,255\}$). Impulsive noise contaminating an image pixel, which is mostly introduced during the image transmission process through a noisy channel, transforms one or more components of its color vector into an extreme value. The classical impulsive noise model described as follows is used in this paper.

Let $\mathbf{F} = \{F_R, F_G, F_B\}$ be the original pixel, let \mathbf{F}^* denote the pixel corrupted by the noise process and suppose that p is the probability of the noise appearance. The image pixels are distorted according to the following scheme:

$$\mathbf{F}^* = \begin{cases} \{d_1, F_G, F_B\} & \text{with probability } pp_1, \\ \{F_R, d_2, F_B\} & \text{with probability } pp_2, \\ \{F_R, F_G, d_3\} & \text{with probability } pp_3, \\ \{d_1, d_2, d_3\} & \text{with probability } p(1 - \sum_{i=1}^3 p_i), \end{cases}$$

$$(1)$$

where d_1, d_2, d_3 are independent and equal to 0 or 255 with equal probability, and p_i , i=1,2,3 determine the probability of appearance of the noise in the image channels.

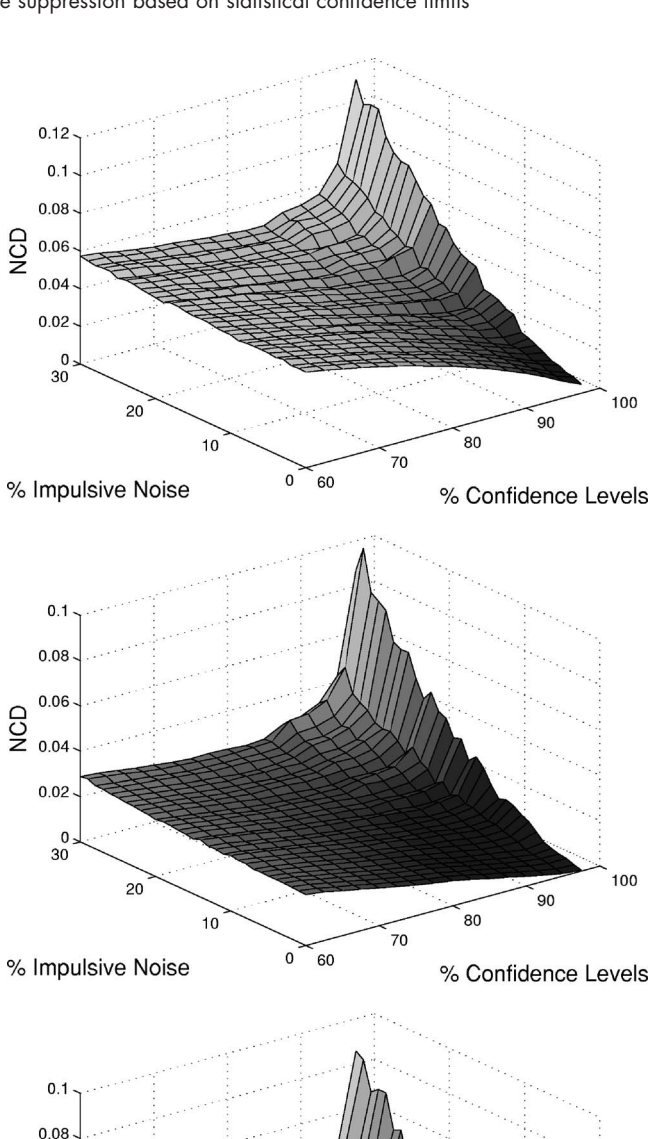
A noisy pixel may break the inner structure of a portion of the image. Impulsive noisy pixel detection could be done by modeling this structure and checking if the pixel in consideration agrees with it or not. This detection is, nevertheless, a challenging task due to edges, corners and fine image details. In this paper, the inner structure of an N-size sliding window $\mathbf{W} = \{\mathbf{x}_i; i=1,2,\ldots,N\}$ (typically N=9 using a 3×3 window) is modeled by a probability distribution estimated from all neighbor pixels of the pixel into consideration.

To estimate the probabilistic distribution of the pixels, the neighbor pixels of the one into consideration, \mathbf{x}_c , are first mean centered and scaled to unit variance. The sample mean (2) and standard deviation (3) obtained are then used to *normalize* the pixel into consideration (4):

$$\bar{\mathbf{x}} = \frac{1}{N-1} \sum_{i=1, i \neq c}^{N} \mathbf{x}_{i}, \tag{2}$$

$$\sigma = \sqrt{\frac{\sum_{j=1, j \neq c}^{N} (\mathbf{x}_{j} - \bar{\mathbf{x}})^{2}}{N - 2}},$$
(3)

$$\mathbf{z}_c = \frac{\mathbf{x}_c - \bar{\mathbf{x}}}{\sigma}.\tag{4}$$



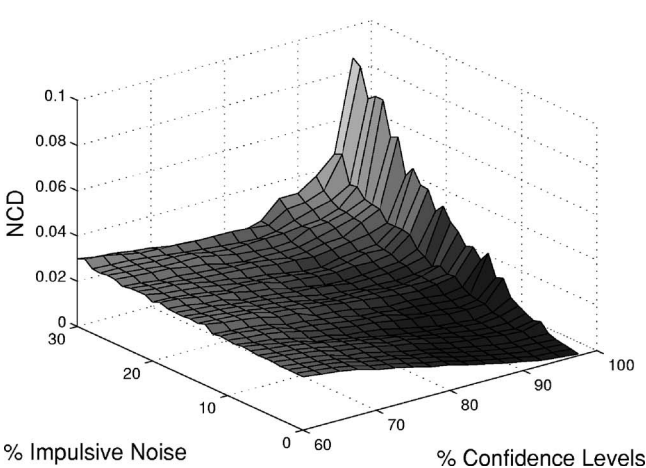
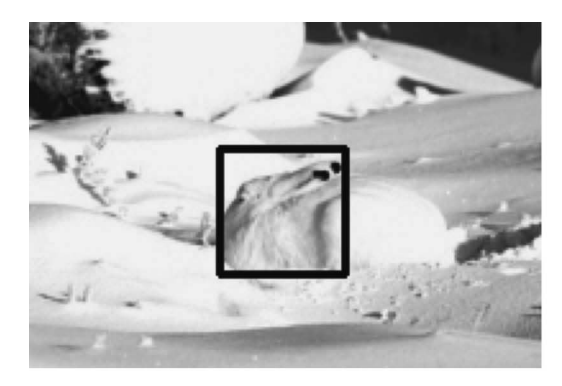


Figure 1. Performance in terms of NCD as a function of the impulsive noise percentage and the confidence level for three test images; see Figs. 2(b)–2(d).

Two strategies for noisy pixels selection are presented in this paper. The first one considers an independent t-student distribution around the mean value for each one of the channels. The second strategy is based on the assumption that the sum of squares of the normalized values of the channels for each pixel follows a squared t-student distribution. The corresponding test is performed on the normalized pixel \mathbf{z}_c and if the value obtained exceeds a prespecified confidence limit, the pixel is filtered. The common assumption underlying both filters is that the values of the pixels are





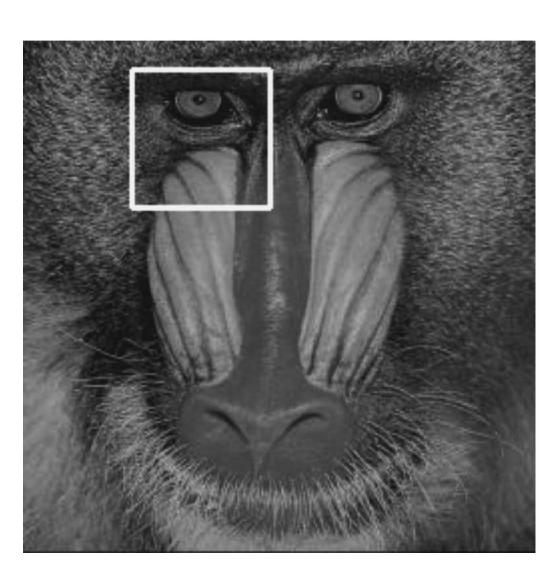




Figure 2. Test images: detail of arctic hare image (copyright photo courtesy of Robert E. Barber), detail of baboon image, detail of Lena image, and detail of peppers image. (Available in color as a Supplemental Material for at least two years from date of publication at www.imaging.org.)

normally distributed around the vector mean of the window. The philosophy of these methods is similar to those in Refs. 22 and 23. The main difference comes from the fact that here a Student's-t or squared Student's-t distribution is assumed for modeling the data.

The proposed selection strategies are used to switch between the identity operation and the VMF operation. Hence, two switching vector filters called t-test vector median filter (tT-VMF) and squared t-test vector median filter (StT-VMF) are defined. Using the notation above, the output of these vector filters is as follows:

$$\mathbf{y}_{tT-VMF} = \begin{cases} \mathbf{y}_{VMF} & \text{if } \exists m \in \{1, 2, \dots, d\} / |z_c^m| > t_{N-2, \alpha/2} \\ \mathbf{x}_c & \text{otherwise} \end{cases},$$
(5)

Table 1. Confidence levels calibrated without information about the percentage of impulsive noise (calibration 1).

	tT-VMF	StT-VMF
Lena	90	75
Baboon	92.5	77.5
Peppers	85	77.5

$$\mathbf{y}_{StT-VMF} = \begin{cases} \mathbf{y}_{VMF} & \text{if } \sum_{m=1}^{d} (z_c^m)^2 > d(t_{N-2,\alpha/2})^2, \\ \mathbf{x}_c & \text{otherwise} \end{cases}$$
(6)

where z_c^m is the value of the mth channel of \mathbf{z}_c , $t_{N-2,\alpha/2}$ is the positive critical value of a Student's-t distribution with N-2 degrees of freedom at a certain confidence level α , ²⁶ and \mathbf{y}_{VMF} denotes the output of the VMF operation.

Table II. Confidence levels calibrated using a vague information about the percentage of impulsive noise (calibration 2).

	†T-VMF			S17-VMF		
	[0-10%](%)	[10-20%](%)	[20-30%](%)	[0-10%](%)	[10-20%](%)	[20-30%]
Lena	95	90	82.5	92.5	77.5	65
Baboon	97.5	92.5	85	97.5	80	65
Peppers	95	90	82.5	90	80	65

COMPUTATIONAL ANALYSIS

Computationally efficient filters are of interest and have been the object of several works.^{27,28} In this section it is shown that the proposed switching filters are fast and more computationally efficient than the classical VMF.

In order to compare the computational efficiency of VMF, tT-VMF and StT-VMF the number of operations to be computed for each image pixel for the VMF and for the proposed filters will be analyzed considering a filtering window W of size N.

In the VMF, for each pixel into consideration, $(N^2-N)/2$ distances have to be calculated first. If the L_1 distance is used, three comparisons and five additions/substractions are to be calculated for each distance. Thus, computing the $(N^2-N)/2$ distances means computing $[5(N^2-N)]/2$ additions/substractions and $[3(N^2-N)]/2$ comparisons. Second, the accumulated distance for each pixel in the filtering window has to be calculated. This means N^2-2N further additions. Finally, the minimum accumulated distance has to be found to determine the filter output. For this, N-1 further comparisons are necessary. So, the VMF has to compute $(3N^2-N-2)/2$ comparisons, and $(7N^2-9N)/2$ additions/substractions.

In the case of tT-VMF, the noisy pixel selection has to be calculated for each image pixel and only for those pixels determined as noisy the VMF operation is performed. The noisy pixel selection means to compute: 3(N-2) additions and one division for calculating the mean value excluding the pixel in consideration; 3N subtractions for subtracting the mean to every pixel in the window; 3(N-1) products, 3(N-2) additions, one division, and one square root for calculating the standard deviation; three divisions for dividing the pixel into consideration by the standard deviation; and finally, three comparisons for determining whether the pixel is noisy or not.

Note that the confidence limit corresponding to a confidence level is fixed for both distributions and it may be precalculated. So, its computational cost is not considered in this analysis.

Two different cases have to be considered: If the pixel is determined as a non noisy pixel then only three comparisons, (9N-12) additions/substractions, 3(N-1) products, five divisions, and one square root have to be calculated; On the other hand, if the pixel is determined as noisy then, in addition to the operations above, the VMF operation has to

Table III. Image-independent confidence levels estimated as the mean of the values obtained from calibration 1 and 2 using the calibration images for each of the merit figures.

	<i>tT</i> -VMF					
	[0-30%]	[0-10%]	[11-20%]	[21-30%]		
NCD	90	95	90	82.5		
MAE	95	97.5	95	92.5		
PSNR	92.5	95	92.5	85		
	StT-VMF					
	[0-30%](%)	[0-10%](%)	[11-20%](%)	[21-30%](%)		
NCD	77.5	92.5	80	65		
MAE	87.5	97.5	87.5	80		
PSNR	77.5	95	77.5	65		

be done. This involves a total of $(3N^2-N+4)/2$ comparisons, $(7N^2+9N+24)/2$ additions/substractions, 3(N-1) products, five divisions, and one square root.

For the sake of simplicity, let us consider a 3×3 filtering window, so N=9 in this case. The VMF computes 116 comparisons and 243 additions/substractions for each image pixel. In the tT-VMF, for the pixels determined as non noisy pixels three comparisons, 69 additions/substractions, 24 products, five divisions, and one square root have to be calculated. For the pixels determined as noisy 119 comparisons, 312 additions/substractions, 24 products, five divisions, and one square root have to be calculated. The following assignment of computational cost units²⁹ (ccu) will be considered for the final computational cost comparison: one comparison=3 ccu; one addition/substraction=3 ccu; one product=3 ccu; one division=7 ccu; and one square root = 10 ccu. Other possible assignments of ccu may be considered and the computational efficiency of the proposed approaches can easily be proof.

Then, the total cost of the VMF operation would be 1077 ccu. In the tT-VMF approach, the non-noisy pixels

Table IV. Mean values obtained from 1% to 30% of impulsive noise and several images. The values for NCD, MAE, and PSNR and the filters tT-VMF and StT-VMF with confidence levels for optimum performance, calibration 1 and 2 are presented. Calibration (above) involves the details of the baboon, lena, and peppers images. Test (below) includes the details of the arctic hare image.

	1T-VMF			StT-VMF		
	NCD	MAE	PSNR	NCD	MAE	PSNR
			Calibration			
Optimum	0.0176	2.1840	30.4478	0.0217	2.5795	29.0024
Calibration 1	0.0205	2.3422	29.2495	0.0259	3.4424	27.4284
	(+16.5%)	(+7.2%)	(-3.9%)	(+19.4%)	(+33.5%)	(-5.4%)
Calibration 2	0.0186	2.1840	30.0128	0.0225	2.8087	28.4851
	(+5.6%)	(+2.4%)	(-1.4%)	(+3.7%)	(+8.9%)	(-1.8%)
			Test			
Optimum	0.0044	1.0862	33.9629	0.0058	1.3503	32.6349
Calibration 1	0.0058	1.1272	32.1541	0.0072	2.0663	30.7119
	(+31.8%)	(+3.8%)	(-5.3%)	(+24.1 %)	(+53%)	(-5.9%)
Calibration 2	0.0048	1.1262	33.1961	0.0065	1.4789	31.3007
	(+9.1%)	(+3.7%)	(-2.3%)	(+12.1%)	(+9.5%)	(-4.1%)

cost would be 333 ccu and the noisy pixel cost would be 1410 ccu. So the tT-VMF would be computationally simpler than the VMF unless at least roughly the 69% of the pixels were determined as noisy.

In the case of the StT-VMF, three products and two additions more than in the tT-VMF are necessary, but only one comparison is done to determine if the pixel is noisy. Then, the non-noisy pixels cost would be 342 ccu and the noisy pixel cost would be 1419 ccu. This approach would be computationally simpler than the VMF unless at least roughly the 68% of the pixels were determined as noisy.

As it could be expected, the computational complexity of the proposed filters depends on the percentage of contaminated pixels. The lower the percentage of contaminated pixels is, the lower the computational complexity.

CALIBRATION OF THE CONFIDENCE LEVEL

The performance of any filtering strategy is assessed using a series of objective quality measures. In this paper, the normalized color difference (NCD), the peak signal-to-noise ratio (PSNR), and the mean absolute error (MAE) are used. These metrics are defined as follows:¹

MAE =
$$\frac{\sum_{i=1}^{N} \sum_{j=1}^{M} \sum_{q=1}^{Q} |F^{q}(i,j) - \hat{F}^{q}(i,j)|}{NMQ},$$
 (7)

$$PSNR = 20 \log \left\{ \frac{255}{\sqrt{\frac{1}{NMQ} \sum_{i=1}^{N} \sum_{j=1}^{M} \sum_{q=1}^{Q} \left[F^{q}(i,j) - \hat{F}^{q}(i,j) \right]^{2}}} \right\},$$
(8)

where M, N are the image dimensions, Q is the number of channels of the image (Q=3 for a RGB color image), and $F^q(i,j)$ and $\hat{F}^q(i,j)$ denote the qth component of the original image vector and the filtered image, at pixel position (i,j), respectively, and

$$NCD_{Lab} = \frac{\sum_{i=1}^{N} \sum_{j=1}^{M} \Delta E_{Lab}}{\sum_{i=1}^{N} \sum_{j=1}^{M} E_{Lab}^{*}},$$
 (9)

where $\Delta E_{Lab} = [(\Delta L^*)^2 + (\Delta a^*)^2 + (\Delta b^*)^2]^{1/2}$ denotes the perceptual color error and $E_{Lab}^* = [(L^*)^2 + (a^*)^2 + (b^*)^2]^{1/2}$ is the *norm* or *magnitude* of the original image color vector in the $L^*a^*b^*$ color space.

The quality measure taken into account in a specific application depends on the nature of that application. When images are filtered previous to human inspection, the NCD measure may be used due to it approaches the human perception. When images are going to be the input of an automatic (in any degree) system (e.g., an image retrieval system), the PSNR or MAE measures may be appropriate.

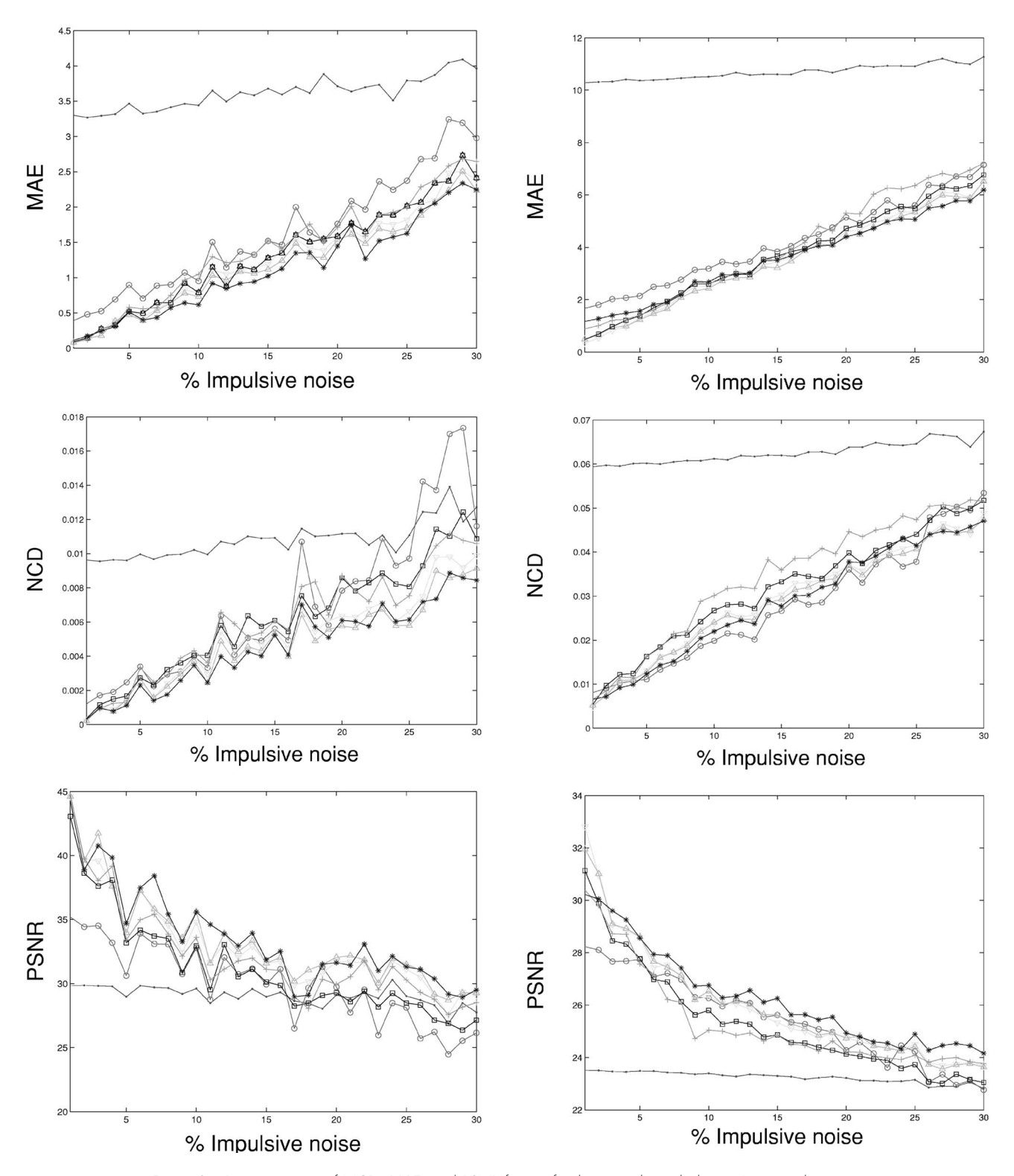


Figure 3. Representation of NCD, MAE, and PSNR figures for the arctic hare, baboon, Lena, and peppers images. The filters used in the comparative are the VMF (dotted lines), the FIVF (lines with squares) (see Refs. 13), the SAMF (lines with circles) (see Refs. 24 and 25), the AVMF (lines with triangles) (see Ref. 22), MAVMF (lines with inverted triangles) (see Ref. 22), and the two filtering strategies proposed in this paper, tT-VMF (lines with stars) and StT-VMF (lines with pluses). (Available in color as a Supplemental Material for at least two years from date of publication at www.imaging.org.)

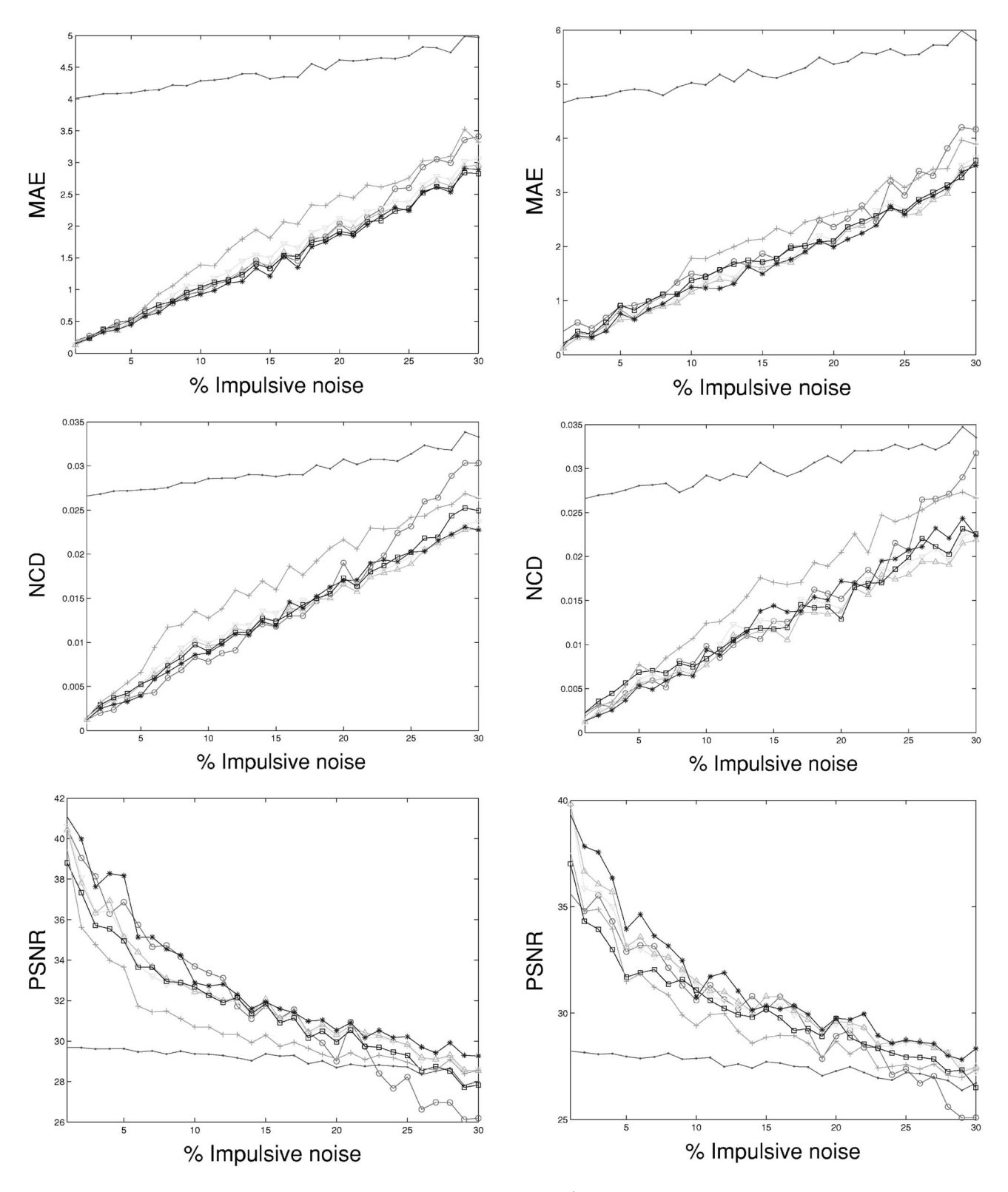


Figure 3. (Continued).

Then, it is reasonable to adjust any filtering strategy by optimizing a specific quality measure.

The performance of the tT-VMF in terms of NCD is shown in Fig. 1 for three test images (see Figs. 2(b)–2(d) as a function of the percentage of impulsive noise from 1% to

30% and the confidence level from 60% to 97.5% (a similar figure could be obtained for the StT-VMF). The figure shows that the performance of the filter depends both on the percentage of noise and the confidence level used. The shape and range of the three surfaces are similar and so a confi-

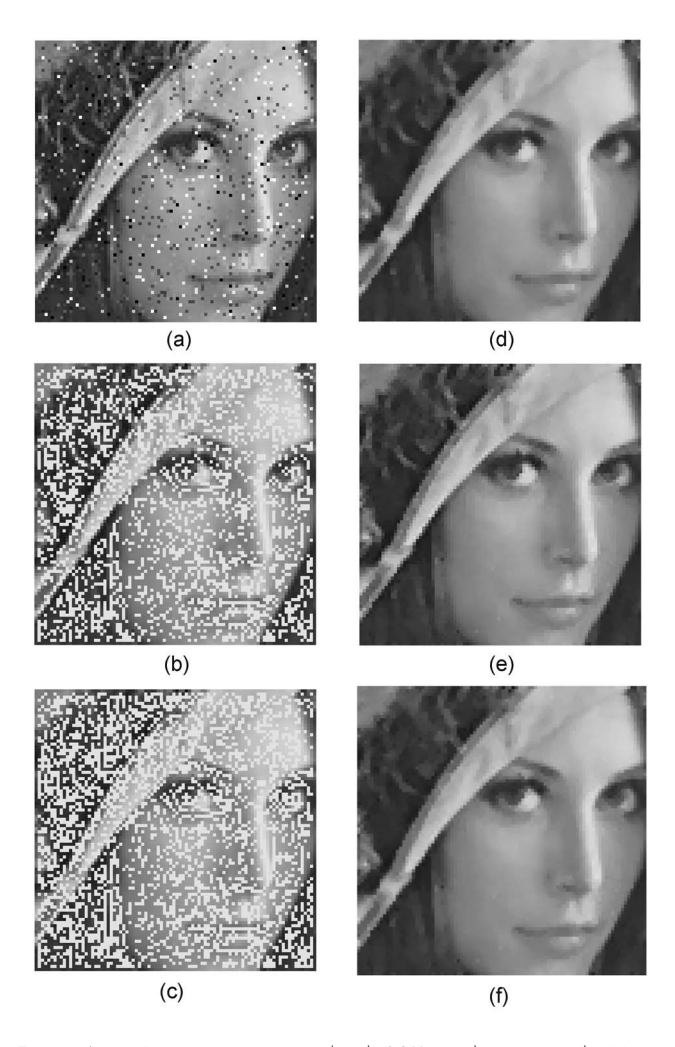


Figure 4. (a) Lena image corrupted with 20% impulsive noise. (b) Number of replaced pixels (in yellow) made by *tT-VMF*. (c) Number of replaced pixels (in yellow) made by *StT-VMF*. (d) Image filtered using the VMF. (e) Image filtered using *tT-VMF*. (f) Image filtered using *StT-VMF*. The percentage of replaced pixels in (b) is 31.46%, whereas it is 38.96% in (c). (Available in color as a Supplemental Material for at least two years from date of publication at www.imaging.org.)

dence level valid for an image may be used to filter another image and a similar performance could be expected.

In order to obtain an appropriate confidence level for any percentage of noise and image, the following two calibration strategies have been considered.

The calibration of the confidence level will be obtained from the details of the baboon, Lena, and peppers images (see Figs. 2(b)–2(d)). These three images have in common that their filtering is complex because of the amount of detail, edges, and rich color set. It has been assumed that the confidence levels obtained may have good performance for other images, even images of different nature. In order to assess the validity of this assumption, the detail of the arctic hare image (Fig. 2(a)) is filtered with the confidence levels obtained in calibration. This image is very different to all the other considered images (with little detail and reduced color set).

As a first step, let us assume there is no information of

the percentage of impulsive noise and that we want to optimize the NCD merit figure (the same procedure will be applied for the MAE and PSNR). In this case, the NCD values for all noise percentages are summed for each confidence level and image. Let $NCD_p^l(I)$ denote the NCD value for the output of the filter when filtering the image I contaminated with p% of impulsive noise using l% as the confidence level. Then, the values $S_l = \sum_{p=0}^{30} \text{NCD}_p^l(I)$, for $l \in \{60,62.5,65,\dots,97.5\}$ are calculated for the different calibration images (it has been observed that values of the confidence level lower than 60% do not present a good performance). A global appropriate confidence level, L, will be that for which $L = \arg \min_{l} S_{l}$. Thus, the appropriate value minimizes the sum of NCD values for all the considered percentages of impulsive noise. The selected confidence levels for each image are listed in Table I. From now on this calibration strategy along with no noise percentage information will be denoted as calibration 1.

On the other hand, the percentage of impulsive noise of an image can be estimated, for instance, using the techniques proposed in Refs. 18, 24, and 25. Nonetheless, it may make no sense to suppose a perfect estimation of the noise percentage. A more realistic approach is to assume the noise percentage is within a certain interval, which can be the case when an estimator is available or when the noise distribution is bounded. Let us now assume the percentage of impulsive noise can be estimated to be in one of the next intervals: [0%-10%], [10%-20%], and [20%-30%]. The confidence levels for every image and interval may be obtained as explained above; (results are shown in Table II). It can be seen the confidence level is inversely proportional to the percentage of noise. From now on this calibration strategy along with the noise estimation mentioned will be denoted as calibration 2.

With any of these assumptions, an image-independent calibration of the confidence level is represented by the mean of the values obtained for the different images. Since the confidence levels included in the experimentation are taken in 2.5% steps, the one nearest to the mean is used. The selected confidence levels appear in Table III. In this table, the values obtained following the same calibration procedure, for MAE and PSNR, are also included.

The quality of both calibrations (without knowledge of the percentage of impulsive noise and with vague approximation of the contaminating impulsive noise) can be assessed in front of the optimum performance of the tT-VMF and StT-VMF. In Table IV, mean values of the NCD, MAE, and PSNR of tT-VMF and StT-VMF, for every image and percentage of noise, are shown. The values between parenthesis are the percentage of worsening of the calibration respect to the optimum performance.

A series of conclusions can be extracted from Table IV. First, reducing the interval of uncertainty of the noise percentage, i.e., improving the estimate of the noise, improves the performance of the calibration. The outcomes of calibration 2 are approximately three times nearer to the optimum performance than those of calibration 1. Second, *tT*-VMF

presents a better performance than *StT*-VMF. Also the calibration for the *StT*-VMF seems to work worse, specially in terms of the MAE. Finally, the confidence levels obtained in the calibration showed a good performance for the test image, giving support to the assumption of image independency.

EXPERIMENTAL RESULTS AND DISCUSSION

The Lena, baboon, peppers, and arctic hare images were corrupted with impulsive noise from 1% to 30% and filtered with the VMF, fast impulsive vector filter (FIVF), ¹³ switching arithmetic mean filter (SAMF), ^{24,25} adaptive vector median filter (AVMF), ²² modified adaptive vector median filter (MAVMF), ²² and the two filtering strategies proposed in this paper, *tT*-VMF and *StT*-VMF. Figure 3 displays the results of each approach.

As it can be seen in Fig. 3, tT-VMF and StT-VMF outperforms VMF. This shows the good performance of the approaches, above all the tT-VMF, even when filtering images of very different nature to those used in the calibration of the confidence levels.

Besides, it can be seen that the tT-VMF outperforms in general terms all the other filters in the case of the arctic hare image. When using the rest of the images (baboon, peppers, and lena, see Fig. 3) the tT-VMF outperforms the rest in terms of PSNR, remaining competitive for the rest of the merit figures.

In Fig. 4(a), a Lena image corrupted with impulsive noise at 20% is presented. The image result of applying VMF (Fig. 4(d)), and the results of the application of the tT-VMF (Fig. 4(e)) and StT-VMF (Fig. 4(f)) are also presented. The images corresponding to the pixels that have been changed by tT-VMF (Fig. 4(b)) and StT-VMF (Fig. 4(c)) are shown as well. For tT-VMF, only 31.46% of the pixels are replaced, whereas this amount increases for StT-VMF up to 38.96%. As it was commented in the Computational Analysis section, tT-VMF and StT-VMF are faster than the classical vector median filter if the amount of replaced pixels is lower than 69% and 68% respectively (see the Computational Analysis section).

On the other hand, as it can also be seen in Figs. 4(d)–4(f), the details are better preserved by tT-VMF and StT-VMF comparing them with the VMF filter. For example, the left eye, the lower part of the nose and some of the hat feathers are better preserved in Figs. 4(e) and 4(f) in comparison to Fig. 4(d).

CONCLUSIONS

In this paper, two strategies to detect impulsive noisy pixels in color images based on statistical confidence limits have been introduced. These strategies have been used to define two switching filters, tT-VMF and StT-VMF, that switch between the VMF and the identity operations.

A strategy to calibrate the confidence level used by the proposed filters has been presented. Results show that this calibration is improved with the estimation of the noise level of a corrupted image. The validity of this calibration method has been tested using an image which is different to those

used in the calibration process, showing that the value of the confidence levels chosen are appropriate.

Furthermore, the performance presented by the *tT*-VMF and the *StT*-VMF is better than the classical VMF, since they are able to better preserve the uncorrupted image structures. Both proposed filters have been compared with recently introduced techniques for impulsive noise removal and the experiments show (Fig. 3) that the *tT*-VMF provides, in general, the best results.

Also, it has been investigated that, in most of the cases, the *tT*-VMF and the *StT*-VMF are faster than the classical VMF since the strategies to detect impulsive noisy pixels are fast and the VMF operation is only applied for those pixels selected by the tests.

Acknowledgments

J.C. and S.M. are funded by the FPU grants program, Secretaría de Estado de Educación y Universidades (Ministry of Education and Science, Spain). The authors would like to thank Dr. Rastislav Lukac for the support of useful material and information.

REFERENCES

- ¹ K. N. Plataniotis and A. N. Venetsanopoulos, Color Image Processing and Applications (Springer-Verlag, Berlin, 2000).
- ²H. A. David, *Order Statistics* (Wiley, New York, 1981).
- ³ P. S. Huber, *Robust Statistics* (Wiley, New York, 1981).
- ⁴ J. Astola, P. Haavisto, and Y. Neuvo, "Vector median filters," Proc. IEEE **78**, 678–689 (1990).
- ⁵P. E. Trahanias, D. Karakos, and A. N. Venetsanopoulos, "Vector directional filters: A new class of multichannel image processing filters," IEEE Trans. Image Process. 2, 528–534 (1993).
- ⁶D. G. Karakos and P. E. Trahanias, "Generalized multichannel image-filtering structure," IEEE Trans. Image Process. **6**, 1038–1045 (1997).
- ⁷R. Lukac, B. Smolka, K. Martin, K. N. Plataniotis, and A. N. Venetsanopoulos, "Vector filtering for color imaging," IEEE Signal Process. Mag. 22, 74–86 (2005).
- ⁸T. Viero, K. Oistamo, and Y. Neuvo, "Three-dimensional median-related filters for color image sequence filtering," IEEE Trans. Circuits Syst. Video Technol. **4**, 129–142 (1994).
- ⁹ R. Lukac, B. Smolka, K. N. Plataniotis, and A. N. Venetsanopoulos, "Selection weighted vector directional filters," Comput. Vis. Image Underst. 94, 1–3 (2004).
- ¹⁰R. Lukac, K. N. Plataniotis, B. Smolka, and A. N. Venetsanopoulos, "Generalized selection weighted vector filters," EURASIP J. Appl. Signal Processing 12/1870–1885 (2004).
- ¹¹ L. Lucat, P. Siohan, and D. Barba, "Adaptive and global optimization methods for weighted vector median filters," Signal Process. Image Commun. 17/509–524 (2002).
- ¹² S. Morillas, V. Gregori, G. Peris-Fajarnés, and P. Latorre, "A new vector median filter based on fuzzy metrics," Lect. Notes Comput. Sci. 3656/ 81–90 (2005).
- ¹³ S. Morillas, V. Gregori, G. Peris-Fajarnés, and P. Latorre, "A fast impulsive noise color image filter using fuzzy metrics," Real-Time Imag. 11, 417–428 (2005).
- ¹⁴ H. H. Tsai and P. T. Yu, "Genetic-based fuzzy hybrid multichannel filters for color image restoration," Fuzzy Sets Syst. 114, 203–224 (2000).
- ¹⁵ R. Lukac, K. N. Plataniotis, B. Smolka, and A. N. Venetsanopoulos, "cDNA microarray image processing using fuzzy vector filtering framework," Fuzzy Sets Syst. 152, 17–35 (2005).
- ¹⁶ E. S. Hore, B. Qiu, and H. R. Wu, "Improved vector filtering for color images using fuzzy noise detection," Opt. Eng. (Bellingham) 42, 1656–1664 (2003).
- ¹⁷ B. Smolka, R. Lukac, A. Chydzinski, K. N. Plataniotis, and W. Wojciechowski, "Fast adaptive similarity based impulsive noise reduction filter," Real-Time Imag. 9, 261–276 (2003).
- ¹⁸ B. Smolka, K. N. Plataniotis, A. Chydzinski, M. Szczepanski, A. N. Venetsanopoulos, and K. Wojciechowski, "Self-adaptive algorithm of impulsive noise reduction in color images," Pattern Recogn. 35,

- 1771-1784 (2002).
- ¹⁹ H. Allende and J. Galbiati, "A non-parametric filter for image restoration using cluster analysis," Pattern Recogn. Lett. 25, 841–847 (2004).
- ²⁰ R. Lukac, "Adaptive vector median filtering," Pattern Recogn. Lett. 24, 1889–1899 (2003).
- ²¹ R. Lukac, "Adaptive color image filtering based on center-weighted vector directional filters," Multidimens. Syst. Signal Process. 15, 169–196 (2004).
- ²² R. Lukac, K. N. Plataniotis, A. N. Venetsanopoulos, and B. Smolka, "A statistically-switched adaptive vector median filter," J. Intell. Robotic Syst. 42, 361–391 (2005).
- ²³ R. Lukac, B. Smolka, K. N. Plataniotis, and A. N. Venetsanopoulos, "Vector sigma filters for noise detection and removal in color images," J. Visual Commun. Image Represent 17, 1–26 (2006).

- ²⁴B. Smolka and A. Chydzinski, "Fast detection and impulsive noise removal in color images," Real-Time Imag. 11, 389–402 (2005).
 ²⁵B. Smolka and K. N. Plataniotis, "Ultrafast technique of impulsive noise
- ²⁵ B. Smolka and K. N. Plataniotis, "Ultrafast technique of impulsive noise removal with application to microarray image denoising," Lect. Notes Comput. Sci. 3656, 990–997 (2005).
- Nomikos and J. F. MacGregor, "Multivariate SPC charts for monitoring batch processes," Technometrics 37, 41–59 (1995).
 M. Barni, F. Buti, F. Bartolini, and V. Capellini, "A quasi-euclidean norm
- ²⁷ M. Barni, F. Buti, F. Bartolini, and V. Capellini, "A quasi-euclidean norm to speed up vector median filtering," IEEE Trans. Image Process. 9, 1704–1709 (2000).
- ²⁸ M. Barni, "A fast algorithm for 1-norm vector median filtering," IEEE Trans. Image Process. 6, 1452–1455 (1997).
- ²⁹ C. Jeong, W. Park, T. Han, and S. Kim, "Cost/performance trade-off in floating-point unit design for 3D geometry processor," in *IEEE Asia-Pacific Conference on ASIC* (IEEE, Piscataway, NJ, 1999), pp. 104–107.